Hydrothermal equalibria and ore formation

Kotova N.P. Experimental study of effect of fluorides concentration and fluid pressure on niobium oxide solubility at T = 550^o C and P = 50 and 100 MPa (Co-CoO buffer).

IEM RAS, Chernogolovka (kotova@iem ac.ru)

Abstract. Nb_2O_5 solubility as a function of fluoride concentration and fluid pressure was investigated in NaF solutions with concentrations from 0.01 to 2 m and LiF solutions with concentrations from 0.01 to 0.1 m at 550 °C and P= 50 and 100 MPa under Co-CoO oxidizing conditions. Comparison of the experiments results on Nb_2O_5 solubility in NaF and LiF aqueous solutions showed that at 550 ° C and P = 50 and 100 MPa the content of Nb is within the limits of $10^{-4} – 10^{-3}$ m. The decrease of fluid pressure from 100 to 50 MPa in NaF and LiF solutions has practically no effect on Nb_2O_5 solubility.

Key words: experiment, oxide niobium, hydrothermal solubility, pressure, fluloride solutions

The development of new forecasting and prospecting criteria of rare metals deposits of Ta and Nb requires a clear understanding of their formation conditions. As is known, there are various hypotheses of the genesis of these deposits - magmatic and hydrothermal- metasomatic. We attempted to look at the problem of these deposits origin taking into account the results of experiments that can provide some geologists new criteria and restrictions on the the interpretation of geological data and to assess the reliability one hypothesis or another [Kotova NP, 2015; Kotova NP, Korzhinskaya VS, 2015]. We carried out experimental study of solubility of niobium oxide (Nb_2O_5) - analogue of a natural mineral nioboxide - in fluoride solutions.

Experiments were performed on a hydrothermal line. The Pt capsules and the container containing the buffer were placed together into cold-seal autoclave of the Tuttle type with a 1 cm diameter cylindrical bore. The pressure was regulated by a Burdon manometer (MP-2500) with a maximum uncertainty of ± 5 bar.

The Nb_2O_5 solubility as a function of fluoride concentration and fluid pressure was investigated in NaF solutions with concentrations from 0.01 to 1 m and in LiF solutions with concentrations from 0.01 to 0.1 m at 550 °C and P = 50 and 100 MPa under Co-CoO oxidizing conditions. The run duration was 18 days at 100 MPa, and 21 days at 50 MPa. Experimental data are shown in Fig. 1 and 2. Experimental results show that the solubility of niobium oxide strongly depends on the fluoride concentration.

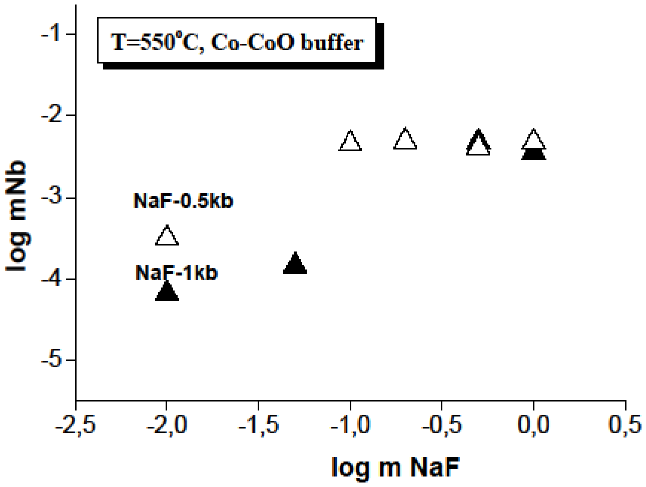

Fig. 1. Effect of the NaF concentration and fluid pressure on the solubility of Nb_2O_5 at T = 550 ° C (triangles - at P = 0.5 kbar, closed triangles - at 1 kb)

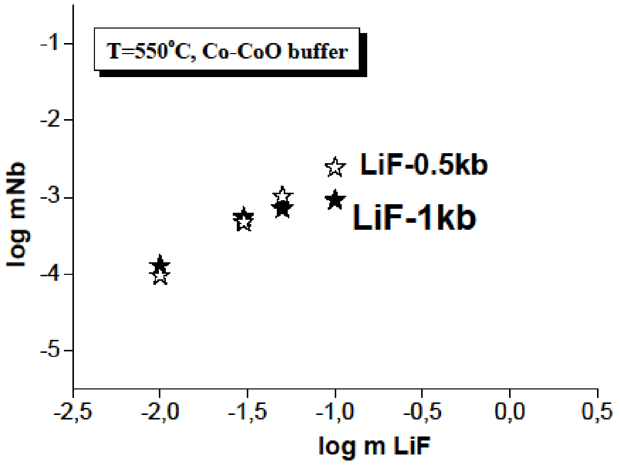

Fig. 2. Effect of the LiF concentration and fluid pressure on the solubility of Nb_2O_5 at T = 550 ° C (stars - at P = 0.5 kbar, closed stars - at 1 kb)

It was established experimentally that the decrease of the fluid pressure in NaF and LiF solutions from 100 to 50 MPa has practically no effect on the Nb_2O_5 solubility. At low concentrations of NaF and LiF (less than 10^{-2} m) the niobium content in the solution is 10^{-4} m. With increasing concentration of the fluorine-ion the Nb_2O_5 solubility increases. It reaches $10^{-2.5}$ m in 1 m NaF and 10^{-4} m in 0.1 m LiF. It is 1.5 orders of magnitude lower than in aqueous solutions of 1 m HF and 1.m KF at the same parameters.

Comparison of the experimental results on the solubility of niobium oxide in NaF and LiF aqueous solutions showed that at T = 550 ° C and P = 50 MPa and 100 dependence of Nb_2O_5 solubility on fluoride concentrations follows the same trends. The niobium solubility in LiF solutions is about 0.5 orders of magnitude lower than in NaF solutions.

Studies have shown that fundamentally important for understanding the genesis of tantalum and niobium deposits is experimentally established fact, which is that hydrothermal transfer of ore metals in amounts sufficient for the formation of industrial concentration, is possible only with concentrated solutions of HF and KF. P-T conditions have little effect on the solubility of niobium and tantalum.

This work was supported by the grants of RFBR 14-05-00424-a, 14-05-00145-a, 14-05-91750-АФ – au, 15-05-03393-a

References:

1. Kotova NP. 2015. Experimental study of Nb_2O_5 solubility in chloride solutions at T = 300 and 550 ° C and P = 100 MPa. Procceding of the All-Russian Annual Seminar of Experimental Mineralogy, Petrology and Geochemistry. Moscow, in 2 vols. Ans. Editor A.A.Kadik - M: GEOKHI RAS, p.
2. Kotova NP., Korzhinskaya VS 2015. Experimental study of the behavior of niobium oxide and natural pyrochlore in fluoride and chloride solutions // In D.: XVII All-Russian meeting of Experimental Mineralogy. Section III- Phase equilibria in silicate and ore systems. Novosibirsk, p.92.

Korzhinskaya V.S., Kotova N.P.

Experimental study of fluid composion (hf+hcl) influence on niobium behavior when dissolving pyrochlore and niobium oxide at T = 550 °C, P = 1000 BAR (Co-CoO BUFFER).

IEM RAS, Chernogolovka vkor@iem.ac.ru; kotova@iem.ac.ru

Abstract. New data on the solubility of niobium oxide (Nb_2O_5) - analogue of natural mineral nioboxide and natural pyrochlore (Ca, Na) 2 (Nb, Ta) 2O6 (O, OH, F) in mixed fluids (HF + HCl) were obtained that allowed to estimate Nb equilibrium content in (HF + HCl) solutions at T = 550 ° C, P = 1000 bar under Co-CoO oxidizing conditions. The initial concentrations of HF varied from 0.01 m to 2 m, while HCl concentration remained constant and equal to 0.5 m. There was comparative analysis of the experimental data on the solubility of Nb_2O_5 and pyrochlore in mixed solutions (HF + HCl) in a concentration range of 0.01 - 2 m with data on the solubility of pyrochlore and Nb_2O_5 in HF and HCl pure solutions l.

Keywords: experiment, pyrochlore, solubility, buffer, chloride.

This experimental study presents some new data concerning the solubility of niobium oxide (Nb_2O_5) - analogue of natural mineral nioboxide and natural pyrochlore (Ca, Na) 2 (Nb, Ta) 2O6 (O, OH, F) in mixed fluids (HF + HCl). The initial concentration of HF varied from 0.01 m to 2 m, while the HCl concentration remained constant and equal to 0.5 m. Experiments were carried out on hydrothermal apparatus of high pressure in sealed platinum capsules using the ampoule technique. The quenched aqueous solutions were analyzed using ICP / MS and ICP / AES (mass spectrometry and atomic emission) methods. The composition of the solid product was characterized using X-ray diffraction and electron microprobe analysis.

Experimental results are presented in Fig. 1, 2 and 3. Comparison of the experimental data on the niobium oxide solubility in fluoride, chloride and mixed fluoride-chloride solutions at 550 ° C and P = 1000 bar (Fig. 1) showed that the addition of Cl- ion to fluoride solutions reduces the niobium oxide solubility by a factor of 1-1.5. Trend dependence of niobium oxide solubility on the concentration of F- ion in the mixed fluoride-chloride solutions occupies an intermediate position between the trends of niobium oxide solubility in pure fluoride and chloride solutions. However, the trends of niobium oxide solubility in fluoride and mixed solutions are comparable at high fluoride concentration (1 and 2 m). The niobium oxide solubility achieves significant values (10-2-10-1 m), that it is sufficient for a real hydrothermal transport of Nb.

Experiments were also carried out on the solubility of natural pyrochlore in mixed solutions. A monocrystal of pyrochlore (Ca, Na) 2 (Nb, Ta) 2O6 (O, OH, F) was selected of weathering crusts from carbonatite deposits Tatarka. It's composition in wt % is Na_2O-7,61%; CaO-14,28%; Nb_2O_5-71,61%; F-5,18%; TiO2-0,83%; Ta2O5≤1%. The concentration dependence of niobium contents on fluoride concentration when dissolving pyrochlore in (HF + HCl) solutions is shown in Fig. 2.

It is established that at low initial concentrations of the mixed solutions (0.01mHF + 0.5mHCl) the niobium equilibrium concentration achieves values $1.66 * 10^{-4}$ mol / kg H_2O. At high concentrations (2 m HF + 0.5 m HCl), niobium equilibrium concentration increases by two orders of magnitude and achieves values $1.33 * 10^{-2}$ mol / kg H_2O. Thus it can be argued that at T = 550 °C and P = 1000 bar, the concentration dependence of pyrochlore solubility in mixed solutions follows positive trend.

Fig. 2 shows also the dependence of the content of Nb in pure HF and HCl solutions obtained earlier [1, 2]. As we can see, m Nb in 0.01 m HF is 2 orders of magnitude lower than in 0.01mHCl and (0.01 m HF + 0.5 m HCl) solution, which can be explained by the high solubility of sodium and calcium present in pyrochlore. However, at high concentrations (1 and 2 m) niobium content sharply increases and becomes higher than in chloride and mixed solutions. The reason may be incongruent solubility of pyrochlore in HCl and (HF + HCl) solutions, where $Na_2Nb_4O_{11}$ and $NaNbO_3$ are formed. Comparison of the experimental results on the solubility of niobium oxide and pyrochlore in mixed fluids (Fig. 3) showed that at low concentrations of fluorides the niobium oxide solubility is about 1 order of magnitude lower than pyrochlore solubility .At high concentrations of F-ion the Nb_2O_5 solubility becomes higher reaching 10^{-1} m in 2 m HF.

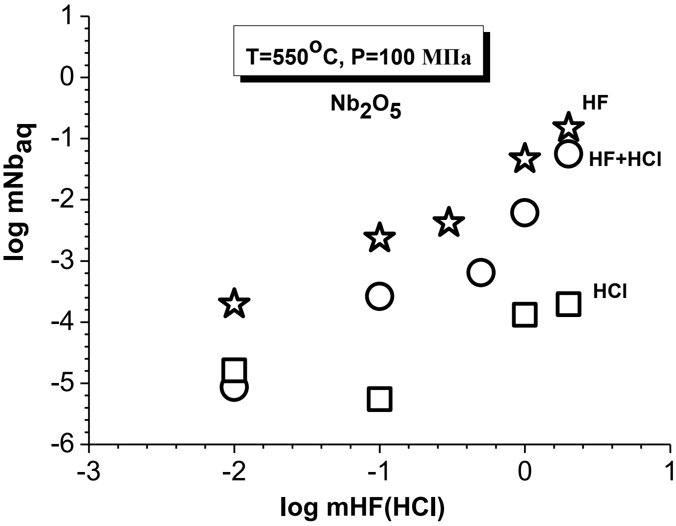

Fig. 1. The concentration dependence of niobium content in the HF, HCl and (HF + HCl) fluids when dissolving niobium oxide at T = 550 ° C, P = 1000 bar (buffer Co-CoO)

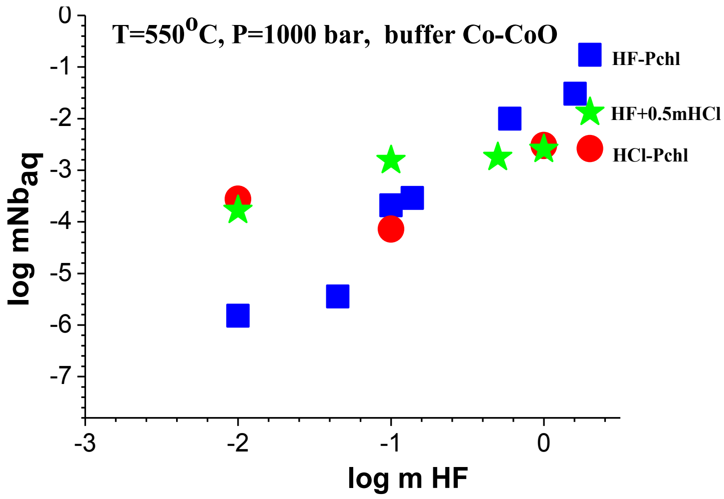

Fig. 2. The concentration dependence of niobium content in HF, HCl and (HF + HCl) fluids when dissolving natural pyrochlore at T = 550 ° C, P = 1000 bar (buffer Co-CoO)

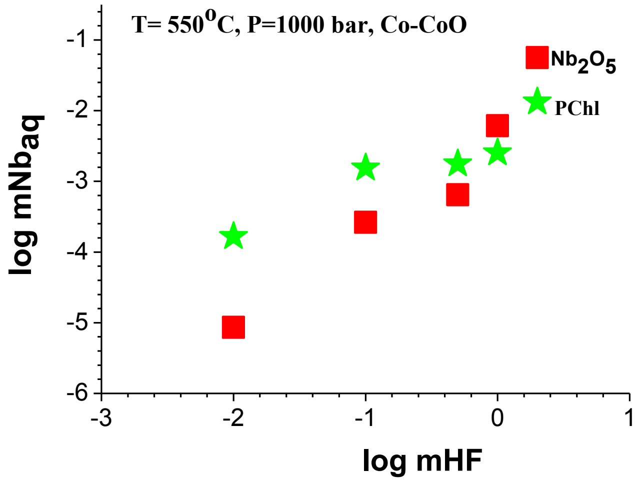

Fig. 3. Concentration dependence of niobium content in (HF + HCl) fluids when dissolving niobium oxide and natural pyrochlore at T = 550 ° C, P = 1000 bar (buffer Co-CoO)

This work was supported by the ONZ RAS program and grants of RFBR 14-05-00424-a and 15-05-03393-a

References:

2.

1. Korzhinskaya VS, Kotova NP(2012). Experimental modeling of possibility of hydrothermal transferring

niobium by fluoride solutions. *Vestn. Otd. nauk Zemle*, 4, NZ9001,doi:10.2205/2012NZ_ASEMPG.

2. Korzhinskaya VS (2013). The influence of chloride concentration on pyrochlore solubility at T = 550 ° C, P = 1000 bar // Experimental Geochemistry, V., №3

Tauson [1,2]V.L., Akimov [1,2]V.V., Spiridonov [1,2]A.M., Budyak [1,2]A.E., Lipko [2]S.V., Smagunov [2]N.V., Arsent'ev [3]K.Yu.

Correlation of experimental and natural (black-shale deposits) data on noble metal speciation and distribution in ore minerals

[1] Irkutsk Scientific Center SB RAS, *e-mail:* vltauson@igc.irk.ru;
[2] Institute of Geochemistry SB RAS,
[3] Institute of Limnology SB RAS

Abstract. The hydrothermal experiments on ore mineral synthesis in presence of noble metals (NM) – Au, Pt, Pd - revealed the well-defined dependences of uniformly distributed modes of the element occurrence on the specific surface area of average crystal in the size fraction. The comparison with ore mineral samples (pyrite, arsenopyrite) from the deposits hosted by black-shale ore formation shows the pattern of NM distribution quite similar to that observed in the experiments. The differences are due to a more complicated history and higher heterogeneity of crystal-forming media in natural systems. The concept of "hidden metal content" is introduced for the elements mainly occurring in superficially bound form as the constituent of nano-sized phases, which avoided further aggregation.

Keywords: hydrothermal experiment, black-shale ore deposits, noble metals, speciation, distribution.

Introduction. The metallogeny of PGE in the deposits of black-shale ore formation represents a complicated problem of ore deposits geology. The experimental methods allow disclosing real NM concentration mechanisms not shaded by the subsequent processes. In recent years, we have observed and studied an interesting natural phenomenon. It implies that a specific superficial layer is formed on the surface of ore mineral crystals growing under hydrothermal conditions. The composition and structure of this layer differ essentially from the crystal volume, and its thickness is usually not more than some hundred nanometers. Due to the features of composition and structure, this layer is capable for the increased trace element uptake, especially, the elements treated as incompatible because of bulk properties of minerals. This phenomenon reveals itself in the experiments as highly determinate dependence of evenly distributed NM content on the size or specific surface area of crystal (Tauson et al., 2011; 2016). While analyzing this dependence it was feasible to determine the contents and ratios of structurally bound and superficially bound modes of NM admixtures.

Experimental Data. Figure 1 exemplifies such dependences in respect to platinum distribution in pyrite and arsenian pyrite with the data of hydrothermal-growth experiments at 500°C and 100 MPa in the solutions based on ammonium chloride. The concentration of superficially bound mode characterizes an average crystal of a number of size fractions, that is, the superficial excess of the element in this crystal. The purpose for using this value is the comparison of the element's content in different modes of its occurrence. It can be seen that the superficially bound element content exceeds that of structurally bound form by an order of magnitude. The existence of these two forms gives rise to the duality of NM distribution coefficient. This is important for solving the reverse problem of modeling, the estimation of NM concentration in the ore-forming fluid.

Natural Data. Similar dependence chacterizes the natural objects. Figure 2 shows the data for pyrite of the gold-ore deposit Degdekan in North-Eastern Russia. This trend seems to be a common feature of Au distribution in many deposits of different genetic types including the gigantic gold-ore deposit Sukhoi Log in East Siberia. However, in this case the dependence is less pronaunced because of the presence of "intrinsic" Au concentrators, carbonaceous micro and nanophases captured under ore pyrite crystallization. A well-defined regularity remains for pyrite from the inter-ore intervals. This evidence indicates that the gold-ore mineralization might not be the result of reaming of the isolated volume of parent sediments only, i.e. the result of auto metasomatism under the action of intrusion heat. It is likely was new fluid that has permiated and reacted with bed rocks. A more complicated hystory and high heterogeneity of the crystal formation medium in nature trigger some other dissimilarities with the experimentally determined trends. Particularly, the fractality of mineral surfaces causes the dualism of the size dependence due to varing capacity for NM uptake by nonautonomous phases of different size levels. Figure 3 demonstrates such a case together with the 3D AFM image of the pyrite crystal surface. This observation thoroughly supports the conception of superficial NM accumulation. The detailed studies with different resolutions verify that the real surface can exceed the topological surface by more than one order of magnitude.The data of X-ray photoelectron spectroscopy and scanning electron microscopy with EDS provide evidence on the elevated contents of La, Os, Ir, Pt, Au and As belonging to the surfaces of the pyrite crystals and shale grains but do not uncover their separated phases or mineral inclusions with platinum-group elements.This may be due to their presence mainly in superficially bound forms composed of nano-sized phases which avoided significant aggregation. This phenomenon can be reffered to as a “hidden metal content”.

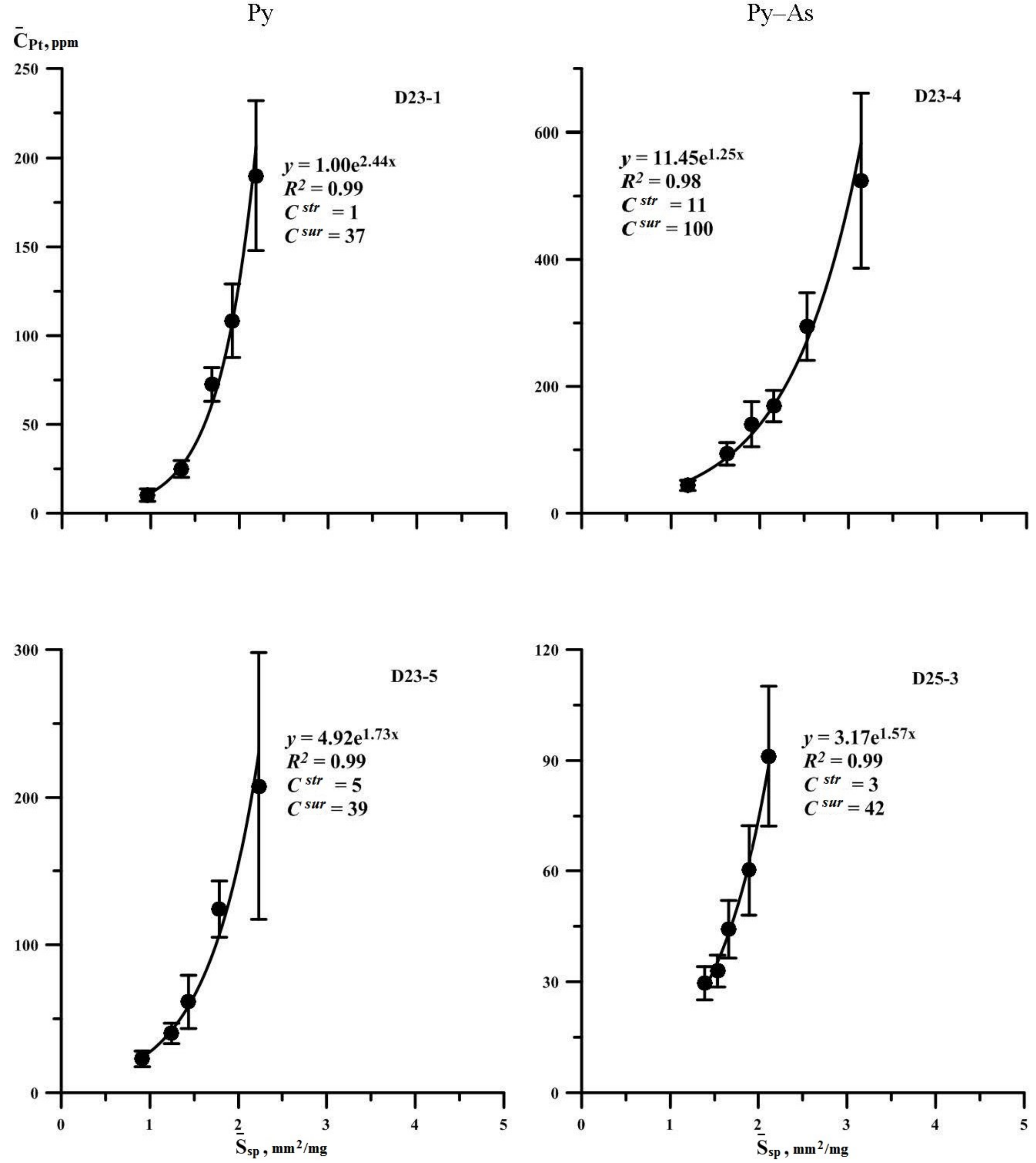

Fig. 1. Dependence of the average concentration of uniformly distributed Pt in pyrite and As-pyrite on the specific surface area of an average crystal in size fractions. C^{str} and C^{sur} are the concentrations of structurally and superficially bound platinum.

Conclusion. Highly determinate exponential dependences of noble metal content on the specific surface area of crystal identified when studying natural objects are principally similar to experimantally obtained ones. Besides, they support the geochemical significance of nonautonomous phases in the distribution of trace elements. It appears that at the black-shale deposits, the “hidden metal content” exists in many cases due to NM composed of nonautonomous phases or the products of their evolution, nano- and micro-sized mineral inclusions. The size dependence of NM content should be taken into account both in the analysis of ore samples and in the development of technologies to recovery ore mineral resources.

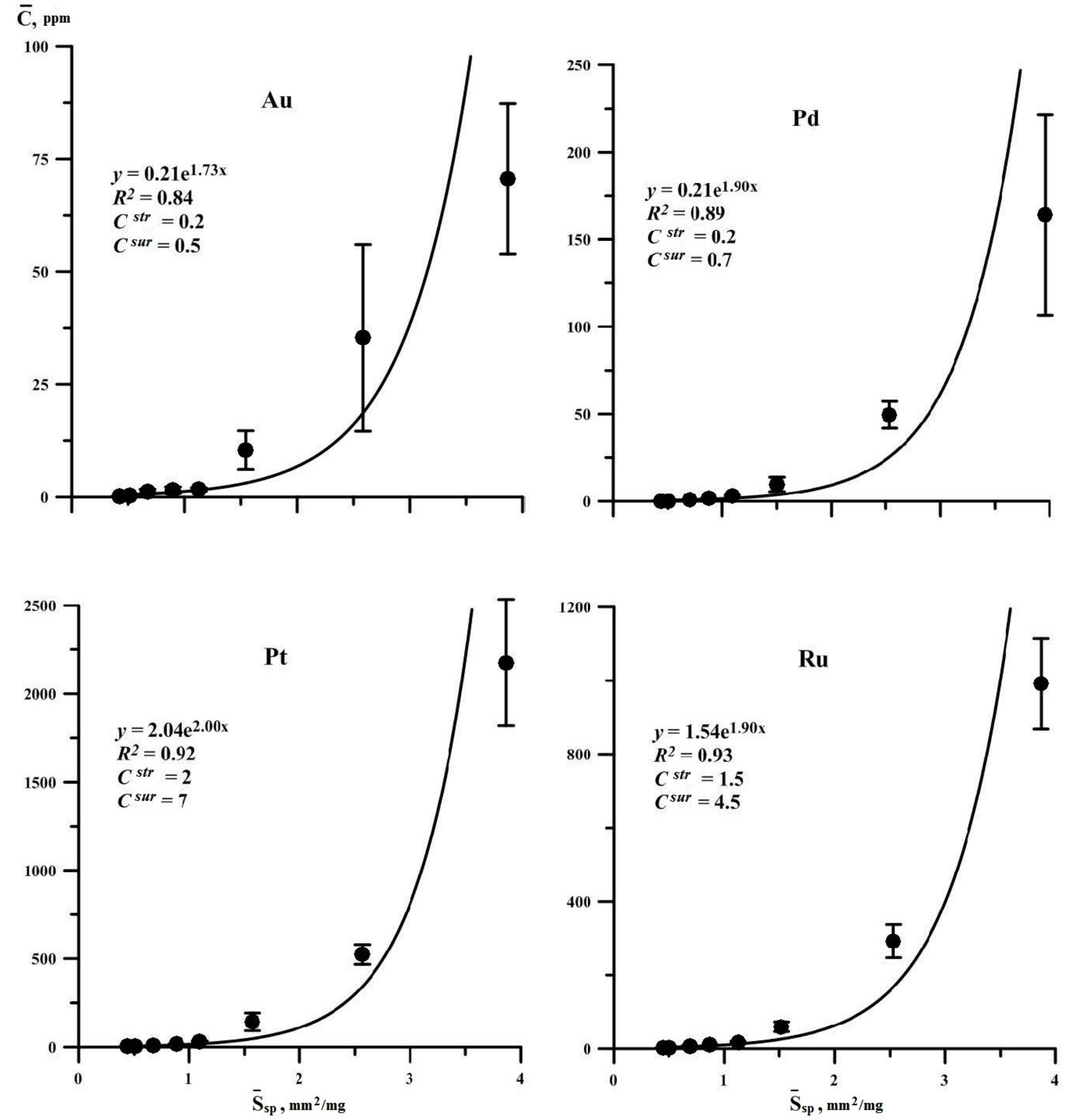

Fig.2. Dependence of the average concentration of uniformly distributed NM in pyrite on the specific surface area of an average crystal in size fractions. The Degdekan deposit.

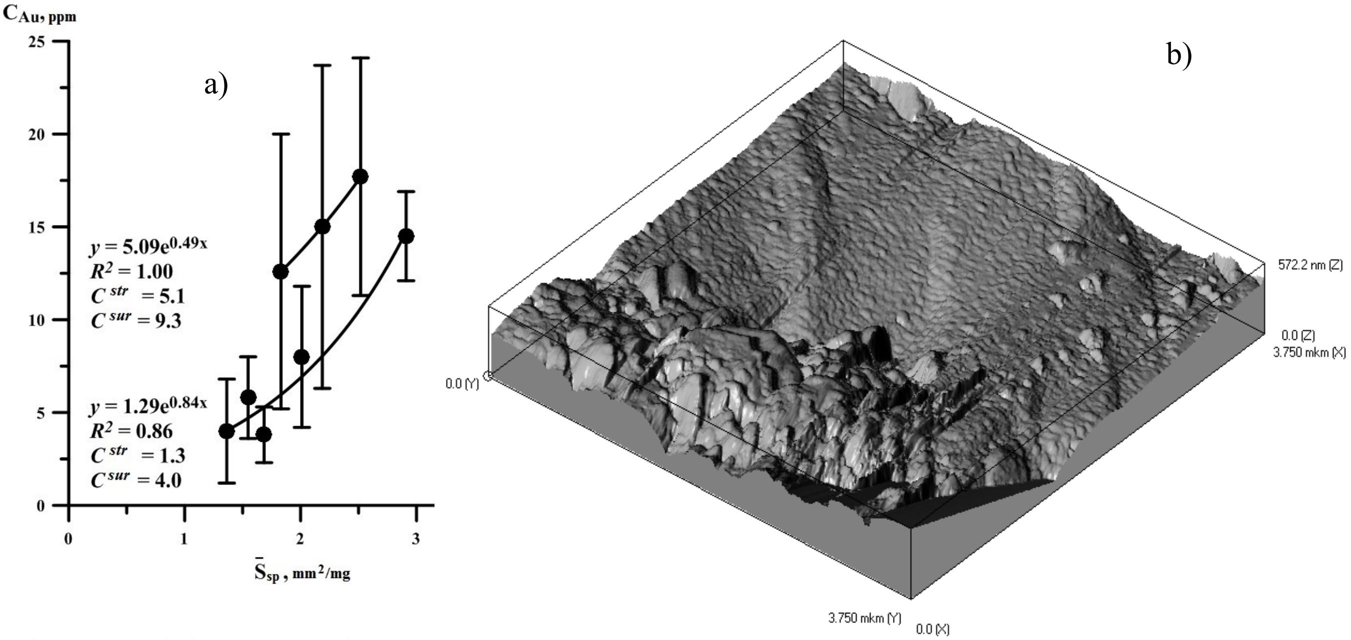

Fig.3. Dualistic trend of Au behavior in pyrite (a) with two types of surface nanostructure shown on the AFM image (b) (3.75x3.75x0.57 μm).

This work is supported by the Irkutsk Scientific Center under Integration Project No.1.3.

References:

1. Tauson V.L., Babkin D.N., Pastushkova T.M. et al. 2011. Dualistic distribution coefficients of trace elements in the system mineral-hydrothermal solution. I. Gold accumulation in pyrite. Geochem. Internat., v. 49, no. 6, p. 568-577.
2. Tauson V.L., Babkin D.N., Pastushkova T.M. et al. 2016. Dualistic distribution coefficients of trace elements in the system mineral-hydrothermal solution. III. Precious metals (Au and Pd) in magnetite and manganmagnetite. Geochem. Internat., v. 54, no.2, p. 149-166.

Tarnopolskaia M.E, Bychkov A.Yu. Experimental study of stability of fluoride iron (iii) complexes in hydrothermal solutions

Geological Department of MSU
mashatarnopolskaya@yandex.ru

Fluoride iron complexes was studied by potentiometric method only at 15, 25, 35°C in (Connick et al., 1956). Therefore, in our study of the iron fluoride complexes experiments was carried out at 86 and 155 ° C. Fluorite solubility was studied in acid solutions with variable concentrations of $FeCl_3$ at 86 and 155°C. For the experiments we used fluorite from Kalanguy deposit. We produced cylinders from a single crystal fluorite (weight about 0.7 g). For experiments we used steel autoclaves with PTFE inserts. Determination of solubility was carried out by the method of weight loss. OptimA program was used for processing the results of experiments. We determined the Gibbs free energy g_T^o for FeF_2^+at 86, 155 ° C, respectively, equal to -645.7 ± 0.3,-645.1 ± 1 kJ / mol. The results are in good agreement with data (Connick et al., 1956) at 15-35°C.

RFBR project 15-05-08110

Akimov V.V.[1], Arsent'ev K.Yu.[2] Behavior of gold nanoparticles in synthetic rock under thermo-gradient hydrothermal conditions

1 -IGC SB RAS, Irkutsk vladlen_akimov@mail.ru, 2-LIN SB RAS, Irkutsk

Abstract. The behavior of gold nanoparticles (NPs) in hydrothermal system «pyrite – quartzite – (graphite + Au NPs) – H_2O» was studied under thermo-gradient conditions ($\nabla T \sim 2$ deg/cm at T=450°C and P=1 kbar). It was shown that the graphitic material does not trap the Au NPs.They however can diffusively migrate in thermo-gradient field and accumulate in the form of micron- and submicron-sized Au particles in pyrite and quartzite.

Keywords: gold nanoparticles, "invisible" gold, synthetic rock, pyrite, quartzite, graphite, hydrothermal systems

Introduction

Until now, the formation and transportation mechanisms of noble metal (MN) nanoparticles (NPs) represent an actual problem in exploring mineralogy and geochemistry of NM deposits. One of them concerns the genesis of “invisible” gold and its relation to the NPs formation. This communication offers preliminary results on the study of NPs redistribution under thermo-gradient hydrothermal conditions. We have employed “synthetic rock” composed of pyrite, quartzite and graphite with Au NPs deposited on graphite surface. The results obtained are presented below.

1 Experimental Technique

The synthetic rock was composed of natural pyrite from the Sukhoi Log deposit, which contained no more than 1-2 ppm Au, super quartzite of the Bural-Sardyk quartzite deposit and finely dispersed graphite powder type MPG-1. Pyrite and quartzite were previously activated mechanically for different time to reach variability in interaction conditions under the same phase composition of experimental system. Au NPs were deposited onto the surface of the graphite powder with magnetron sputtering of gold target. The synthetic rock was prepared as a five-layer sandwich; three of them were the Au NPs-bearing graphite layers separated by pyrite or quartzite layers ($||C+Au||-||FeS_2||-||C+Au||-||SiO_2||-||C+Au||$. The experiments were conducted under hydrothermal conditions in the gold ampoule 12 cm high at linear temperature drop 20 oC at 450oC in the hot zone and 1 kb pressure during 6 days (one day to reach experimental parameters).

2 Methods of Analysis

To study the morphological and size features, as well as chemical composition of the products, the following analytical techniques were used: transmission electron microscopy (TEM), scanning electron microscopy (SEM), electron microprobe analysis (EMPA), X-Ray diffraction (XRD), and energy dispersive spectrometry (EDS) for elemental analysis with EM.

3 Results and Discussion

Graphite. As it is evident from TEM and XRD data (Figures 1 and 2), the Au NPs obtained by magnetron sputtering and deposited onto the graphite powder varied in diameter from 5 to 20 nm. After the hydrothermal treatment, only small part of Au remains as NPs, a major part forms the micron- and submicron Au particles, as TEM, SEM and XRD have showed. Separate Au particles are close to sphere by form; they vary in size from 300 nm up to 1 µm. Besides, the Au particles have perfect crystal structure, as it was found by analyzing the X-ray diffraction patterns: the broadening of XRD peaks of Au microparticles is significantly lower than that of Au NPs (Fig. 2). The EDS analysis indentified that the gold content in these particles ranges from 30 up to 75 wt.% (high dispersion is due to small sizes of the particles, for which the area of signal excitation is larger than the particle itself, and the effect of the graphite background radiation appears).

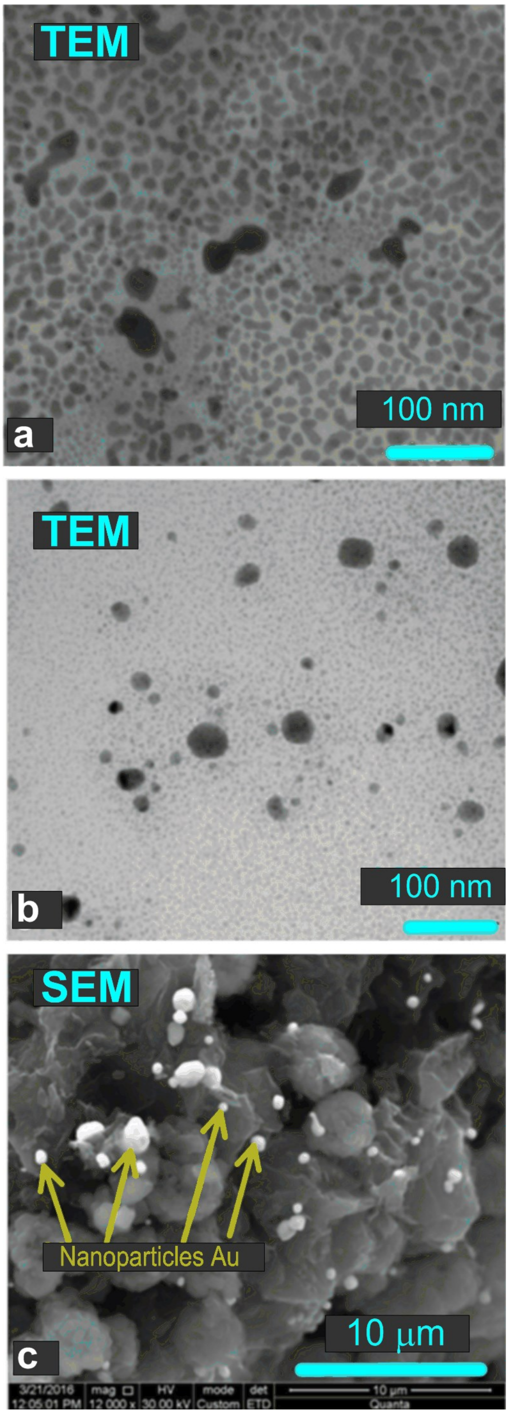

Fig. 1. Starting graphite material with Au NPs (a), nano- and microparticles of Au which have formed on graphite after hydrothermal treatment (b and c, accordingly).

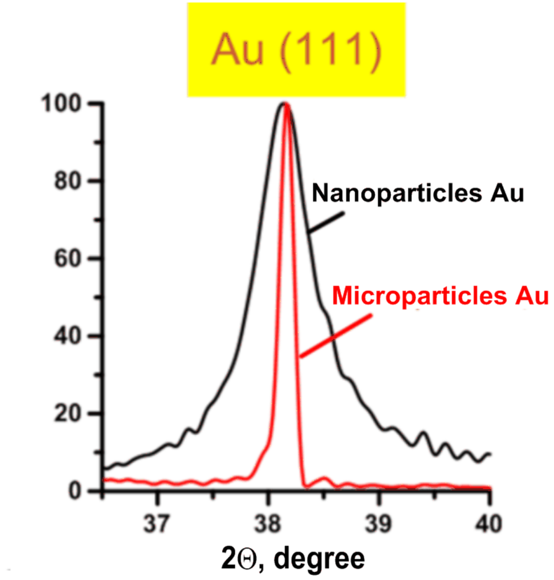

Fig. 2. XRD line profile (111) of Au on graphite before (black line) and after (red line) hydrothermal treatment.

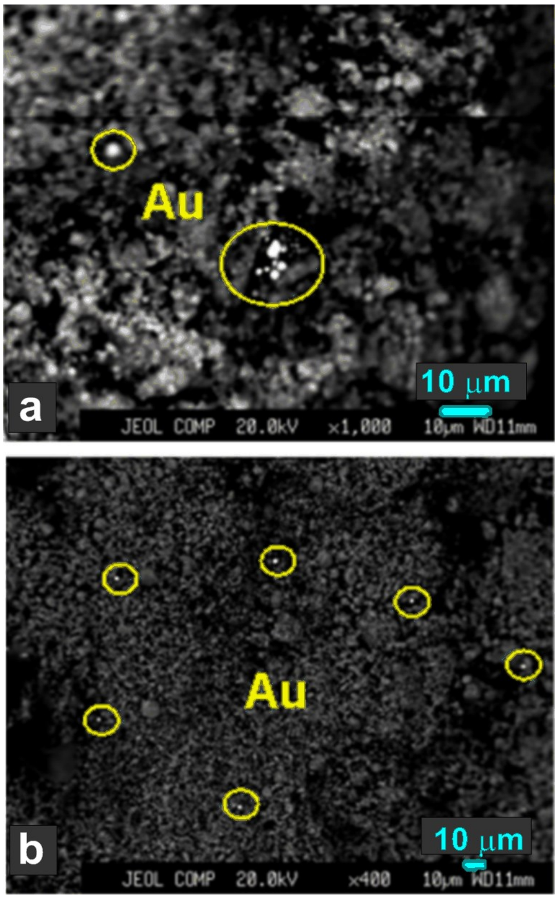

Fig. 3. Pyrite (a) and quartzite (b) with Au microparticles after the hydrothermal treatment. EM images (back-scattered electron mode).

Pyrite and Quartzite._After the hydrothermal treatment, the micron-sized particles containing from 10 up to 85 wt.% Au are observed in pyrite and quartzite by EMPA (Fig. 3). They are mostly round-shaped and comprise some other elements of the system (C – 0-40 wt.%, Si- 0-45 wt.%, O- 0-14 wt.%, Fe- 0-53 wt.%, S-0-34 wt.%). Therefore, Au is transferred both in the form of nano- and microparticles(at Au concentrations close to 85 wt.%) and at the expense of migration of micron-size particles of graphite, pyrite and quartzite in thermo-gradient field.

Conclusions

1 Under the hydrothermal treatment (T=450°C, P= 1 kb) Au NPs are unstable on the graphite surface and form the micron-size particles by the mechanism of block-attachment growth.

2 Under thermal-gradient conditions, Au is transported both in the form of nano- and microparticles of gold itself and together with submicron particles of graphite, pyrite and quartzite on their surfaces.

3 Au microparticles are concentrated in pyrite and quartzite.

This work is supported by RFBR under grants №16-05-00406; №16-35-00102 and Irkutsk Scientific Center under Integration Project No.1.3.

Arsent'ev K.Yu.[1], Voronova I.Yu.,[2] Lipko S.V.,[2] Tauson V.L.[2] Evolution of small-size phases on the surface of pyrite crystals in the system FeS_2 – Ag - Pt.

[1] *LIN SB RAS, IGC SB RAS, Irkutsk* (arskir@gmail.com); [2]*-IGC SB RAS, Irkutsk* (*ivoronova@igc.irk.ru*, *slipko@yandex.ru*, *vltauson@igc.irk.ru*)

Abstract. During the experimental study of the duality of precious metal distribution coefficients between the minerals and fluids, we observed a significant enrichment of the surface of pyrite crystals in Ag and Pt. SEM-EDS and SPM, used in conjunction with EPMA, LA-ICP-MS and XPS, provide information on the evolution of non-autonomous phases (NAP), evenly distributed over the surface and enriched in Pt and other incompatible elements. They evolve in the direction of the intermediate objects (mesophases) of submicron to first microns in size, the composition of which is largely inherited from precursors - the nanoscale NAP. The findings suggest the need for careful attention to the so-called microminerals, widely represented today as new mineral species diagnosed by local methods, without serious analysis of their history.

Keywords: precious metals, non-autonomous phase, hydrothermal experiment, pyrite

Introduction

The distribution coefficient (D) of element in heterogeneous systems such as mineral-melt or mineral-fluid (solution) is one of the important geochemical constants. It is this factor is used in the judgments about the compatibility or incompatibility of elements in varying mineral matrix, in explaining the common geochemical paths of different nature elements or separating elements of similar chemical nature. However, when using D, one should take into account that it is subjected to significant changes with variations of parameters. Especially important is the confidence that we correctly imagine the history of the behavior of an element in one or another mode of its occurrence until the act of determining by any analytical method. This is not trivial. For example, recently in the minerals and rocks are increasingly finding nanoparticles that can camouflage the structurally bound (including isomorphous) form of element, if using in the study of mineral only bulk methods or methods with inadequate spatial resolution.

In our report, the system FeS2–Ag-Pt is taken as an example to demonstrate the role of surface phases in the formation of small-size objects and the D change mechanism due to their influence.

Experiment and methods

Pyrite crystals were synthesized in the presence of Ag and Pt under thermogradient conditions by the conventional hydrothermal method at 500-515°C and a pressure of 1 kbar in ammonium chloride-based solutions. Synthesis was combined with internal sampling. The trapped fluid sample is analyzed after full recovery from the trap by atomic absorption spectrometry (AAS) (for Pt - after preliminary extraction concentration). Experiments are performed in inserts made of titanium alloy VT-8, passivated in boiling nitric acid. Cooling rate under the autoclave quenching in cold running water was ~ 5 Kps. The crystals were studied with AAS method in version SSADSC (statistical selections of analytical data on single crystals), SEM-EDS, AFM, XPS (surface), EPMA, LA-ICP-MS.

Results and discussion

Both impurity elements - Ag and Pt in pyrite are poorly studied. It is considered that pyrite may contain up to 230 ppm Pt probably partly included into the solid solution composition. The incorporation limit of Ag in the pyrite structure is evaluated very ambiguously - from 5 to 1200 ppm (Abraitis et.al, 2004.). Our attempts to find the distribution coefficients of Pt and Ag between pyrite and hydrothermal solutions in the literature failed.

The highly determinate dependences of the content of uniformly distributed form of element on the specific surface area of average crystal in size selection were obtained for Pt. This allowed to determine the dual coefficients of Pt distribution between pyrite and fluid as 21 for structural form and 210 for surface-bound form. For silver, the bulk contents of which were 2 orders of magnitude higher than Pt, a more or less precise size dependences were obtained only in 4 of 7 experiments. These indicate volumetric content of Ag in pyrite at the level of 500-1500 ppm. However, both EPMA and LA-ICP-MS analyses showed an extremely inhomogeneous distribution of Ag. EPMA indicates the Ag content in the pyrite matrix below the detection limit (0.15 wt.%) and the presence of silver phase inclusions - sulfide Ag (I) and proustite with admixture of dervillite end member (in experiments with As).

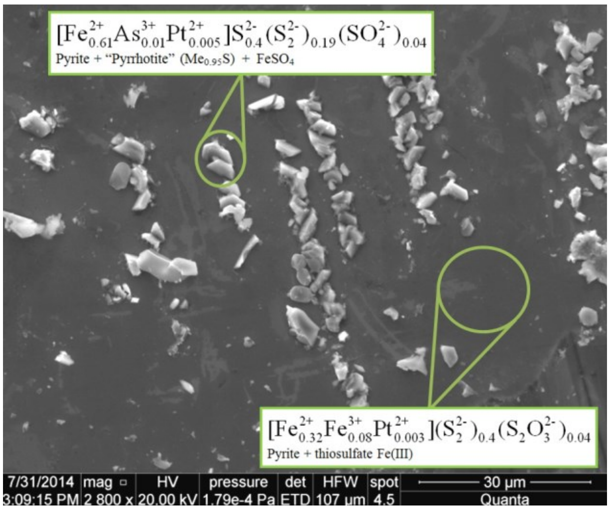

Fig.1. Rows of pyrrhotite-like phase crystals at the pyrite surface. Compositions are calculated on the base of SEM-EDS data accounting for the XPS data (sulfur speciation) and the requirements of electrical neutrality.

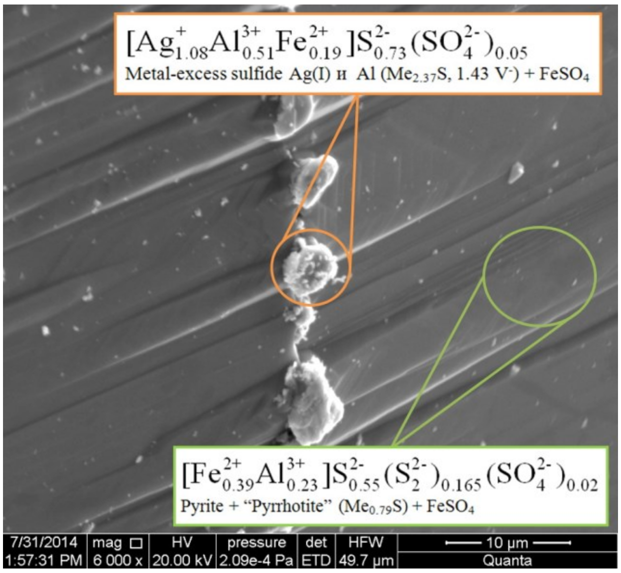

Fig.2. The chain of crystals of metal-excess Ag and Al sulfide along the crack. The composition of the "clean" surface reflects NAP also enriched in Al.

LA-ICP-MS shows a wide range of content of Ag - from 0.n up to the first of thousands of ppm. The obtained data and further studies by electron microscopy lead us to the conclusion that the solid solution of Ag in pyrite exists to about 0.15 wt.% Ag at 500 °C, but cannot be quenched. The system obedience to the principle of continuity of phase formation (Tauson, 2009) leads to the fact that the precursors of bulk phases appeared on the surface - nanoscale non-autonomous phases (NAP) - gradually change the composition with the formation, ultimately, of the heterogeneous surface nuclei of stable bulk phase. We have found that the bulk phase precursors (or mesophases) succeed the features of the chemical composition of NAP. The mesophase formed during aggregation of non-autonomous phases represents "pyrrhotite" with high concentrations of incompatible elements - Al, Ag, Pt, As, etc. Its composition is largely inherited from precursors - nanoscale NAP (Figure 1). "Pyrrhotite" composition varies from $Me_{1.03}S$ to $Me_{0.76}S$. Silver realizes from NAP as far as its thickness increases and diffusive connection of NAP internal layers with supersaturated solution disturbs (Tauson et al., 2014). This gives rise to the formation the own Ag microphases if there is enough free space available, or Ag can diffuse to the surface (Figure 2). The so-called "facilitated diffusion paths" will be provided because the NAP layer is a few hundred nanometers thick. Therefore, the formation of microphase based on Ag occurs near defects - cracks, pores, dislocation surface exposures (nearby etch pits).

The problem of aluminum remains unsolved. Its occurrence caused by the presence of Al in the alloy VT-8, it almost not included in the volume of crystals. Apparently, Al may be incorporated into the surface NAP composition for compensating the negative charge excess of sulfur (S-II instead of S-I in pyrite).

Conclusion

Phase and chemical evolution of non-autonomous phases, involved in the process of crystal growth, leads to the enrichment of pyrite surface by incompatible elements - Ag, Pt, and others. They may be incorporated into the sub-micron and micron-size mesophases, which are the precursors of autonomous mineral inclusions on the surface. Such phases can be erroneously adopted as representatives of new mineral species in natural objects.

This work was supported by RFBR grants №№ 16-35-00102, 15-05-05767, 15-05-00612

References:

1. Abraitis P.K., Pattrick R.A.D., Vaughan D.J., 2004. Variations in the compositional, textural and electrical properties of natural pyrite: a review // Int. J. Miner. Process. V.74. P.41-59.
2. Tauson V.L., 2009. The principle of continuity of phase formation at mineral surfaces // Doklady Earth Sci. V.425A. No.3. P.471-475.

3. Tauson V.L., Lipko S.V., Smagunov N.V., Arsent'ev K.Yu., Loginov B.A., 2014. Influence of surface nanophases on the processes of crystal formation in multiphase mineral systems // Doklady Earth Sci. V. 455.Part 1. P. 317-322.

Popova[1] Y.A., Bychkov[1] A.Yu., Matveeva[1] S.S., Bychkova[2] Ya.V. Geochemical features of lanthanides behavior at the formation of tungsten deposits

[1] Lomonosov Moscow State University; [2] IGEM RAS
julka_p@rambler.ru

Monofractions of minerals and rocks of Spokoyninskoye deposit (Transbaikalia) were analyzed. The content of rare earth elements (REE) have been determined by ICP-MS method. REE concentrations in hydrothermal solutions in equilibrium with fluorite , wolframite and scheelite were estimated based on the distribution coefficients (Raimbault, 1985) .

The contact hornfels are relatively enriched in LREE (La/Lu 25 – 51), Eu minimum is poorly expressed (Eu/Eu* 0.7 – 0.8). In two samples, a positive Ce anomaly is observed, which is characteristic of sedimentary rock. The total REE content in these samples ranges from 163 to 194 ppm. The spectra of greisenized granites are characterized by strongly Eu minimum (Eu/Eu* 0.2 – 0.3) and by prevalence of LREE over HREE (La/Lu 30 – 80). Monazite (Ce, La, Nd…)[PO_4] is the main concentrator of REE in the original granites, and to a lesser extent – xenotime YPO_4 (Distler, 1967).

Wolframites spectra shows two groups by the REE content. The first group includes the spectra of greisenized granites and quartz-wolframite veins, which form a compact group. The total REE content in them is about 180 – 200 ppm. Wolframites of this group are characterized by low content of LREE (La/Lu = 0.03 – 0.4). This is explained by REE concentration of ore-bearing solutions. Fluorites from granites and quartz-tungsten veins are characterized by low content of REE (0.24 – 0.38 ppm) and by the prevalence of HREE over LREE (La/Lu 0.24 – 1.33). Fluorite from quartz-albite-muscovite nodules is characterized by a high content of REE (470 ppm) and there are enriched by cerium group REE (La/Lu=128). The REE content of wolframites and fluorites is controlled by monazite solubility in hydrothermal solutions of Spokoyninskoye deposit. Wolframites and fluorites from quartz-muscovite-albite nodules is characterized by a high content of concretions of light rare earth elements due to the increase of monazite solubility by the formation of alkaline metasomatic rocks.

This work was supported by RFBR, project 15-05-0550.